

Secondary Recrystallization Mechanism of Grain Oriented Electrical Steels

Weimin Mao^{1,2}

(1. School of Materials Science and Engineering, University of Science and Technology Beijing, Beijing 100083, China;
2. School of Materials Science and Engineering, Inner Mongolia University of Science and Technology, Baotou 014010, Inner Mongolia, China)

Abstract: In response to the various doubts currently existing in theory, the process of orientation evolution in the production of grain oriented electrical steel has been comprehensively reviewed. Ultimately, the mechanism of secondary recrystallization was fully elucidated. Only a small fraction of those Goss grains that formed in the surface layer of the hot band during hot rolling under large pass reductions can survive the heavy cold rolling and are further enhanced through subsequent recrystallization annealing. The nucleation process based on polygonization results in recrystallized Goss grains that do not have the size advantage over non-Goss grains. The molar volume expansion effect that occurs during the precipitation of inhibitors such as MnS and AlN in ferrite forces the precipitated particles to maintain a dispersed distribution and hinders the growth behavior of all grains. However, the molar volume expansion effect of the steel sheet near the free surface area will be significantly weakened, resulting in an obvious decrease in particle density due to the opportunity for coarsening of the inhibitor particles in the area. As a result, the surface grains exhibit a growth advantage over the internal grains. Especially at high temperatures, the strong elastic anisotropy of ferrite leads to a higher density of inhibitor particles in the surface Goss grains than in non-Goss grains. Therefore, when the surface grains begin to grow, the speed of grain boundary migration towards Goss grains is significantly lower than that towards non-Goss grains. As a result, while the grain size inside the steel remains basically unchanged, some Goss grains gradually become the largest among all surface grains. As the temperature of the secondary recrystallization annealing increases and the inhibitor particles gradually dissolve back into the ferrite, the surface Goss grains, which are already the largest in size, engulf all grains and complete the secondary recrystallization process characterized by abnormal growth. It is the molar volume effect of inhibitors and the strong elastic anisotropy of ferrites that lead to the abnormal growth of Goss grains originating from the surface layer of hot band during secondary recrystallization.

Keywords: grain oriented electrical steel; orientation evolution; Goss grains; abnormal grain growth

CLC number: TG142.1

Document code: A

Article ID: 1005-9113(2026)00-0000-09

0 Introduction

Grain Oriented (GO) electrical steel, an extremely important electromagnetic material, has been widely produced and used for nearly a century. The key to its excellent magnetic properties lies in the formation of an extremely strong $\{110\} \langle 001 \rangle$ Goss texture in the final secondary recrystallization production process, during which only $\{110\} \langle 001 \rangle$ oriented grains i.e., Goss grains can grow abnormally in size to several tens of times the thickness of the steel sheet^[1]. However, despite long-term research, it is still widely recognized that the mechanism of the

corresponding secondary recrystallization has not been fully clarified so far. The first main challenge faced by this mechanism is that the size of Goss grains is often not larger than the surrounding grains before the start of secondary recrystallization^[2], and therefore does not meet the basic conditions for Goss grain growth^[3]. Various theories attempting to explain the abnormal growth of Goss grains focus on the migration characteristics of grain boundaries in the early stage of secondary recrystallization under the inhibition effect of a large number of second phase particles, including the theory of coincident site lattice boundaries^[4], high-energy boundary theory^[5], the theory of solid-state grain boundary wetting^[6], etc. It is well known

that the inhibition effect of the fine dispersed particles that always exists during the main stage of the secondary recrystallization annealing^[7] is a key factor leading to the secondary recrystallization behaviors, and only considering the early migration characteristics of grain boundaries cannot really reveal the complete mechanism, which becomes the second main challenge of the current theories. It should be recognized that in order to fully reveal the mechanism of abnormal growth of Goss grains during secondary recrystallization, it is necessary to track the evolution of Goss grains throughout the entire production process of GO steels, rather than just focusing on the secondary recrystallization annealing process.

1 Formation of Initial Goss Texture in the Surface of Hot Rolled Band

Research has confirmed^[8] that Goss grains that are able to grow abnormally are mainly located near the surface layer of the hot rolled band of GO steels, while non-Goss grains near the surface usually do not grow abnormally. If the surface layer of the hot band is removed, there will be no abnormal grain growth during the final high-temperature annealing process, even if there is a small number of Goss grains in the central layer of the steel sheet, they cannot grow

abnormally. In view of this, the Goss grains in the surface layer of hot band are the initial source of strong Goss texture, which is inevitably observed in conventional GO steel (for example, Fig.1 (a)) and high magnetic induction GO steel (for example, Fig.1 (b)) from industrial processing, and there must be a mechanism for their stable existence.

The basic composition of GO steel maintains ferrite as its main phase structure, even in very high temperature ranges, so hot rolling deformation mainly involves the deformation of ferrite. In the later stage of the hot rolling process of GO steel, lower hot rolling temperature and very fast deformation rate result in little dynamic recrystallization in the hot band, including in the surface layer, which leads to mainly un-recrystallized deformation structure of the hot band^[9]. As is well known, rolling deformation mainly leads to the formation of textures such as $\{111\} \langle 110 \rangle$, $\{111\} \langle 112 \rangle$, $\{112\} \langle 110 \rangle$, and $\{001\} \langle 110 \rangle$ within the steel sheets (Fig. 1 (c))^[10]. However, these textures were not observed in the surface of the hot band of GO steel, but mainly $\{110\} \langle 001 \rangle$ and $\{112\} \langle 111 \rangle$ textures (Figs. 1 (a) and 1 (b)), in comparison with Fig.1(c)) that should not be stable during the rolling process, and it is difficult to clarify the reasons for formation of these textures using existing plastic deformation crystallography theories.

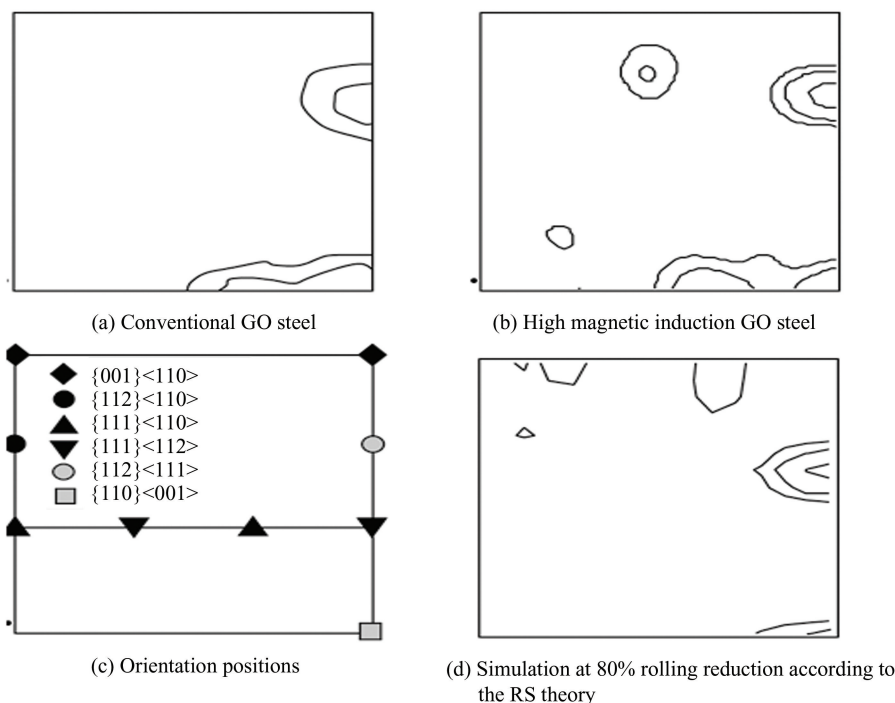


Fig.1 Hot band textures in surface layer of industrial GO steels and the corresponding simulation ($\varphi_2 = 45^\circ$ ODF sections, density levels: 2, 4, 8, φ_2 is the Euler angle in orientation space.)

The $\{110\} \langle 111 \rangle$ systems of ferrite are most prone to slip, making it the main crystallographic mechanism of ferrite plastic deformation. In addition, the $\{112\} \langle 111 \rangle$ and $\{123\} \langle 111 \rangle$ systems can also be activated, which is usually considered to be achieved through regular cross slip among different $\{110\} \langle 111 \rangle$ systems at a fixed ratio^[1,11]. This repeated cross slip can avoid excessive work hardening induced by simple $\{110\} \langle 111 \rangle$ continuous slip without cross slip, ensuring the smooth implementation of the plastic deformation process^[9]. The combination of different slip systems on the $\{110\}$, $\{112\}$, and $\{123\}$ planes will result in the formation of rolling textures such as $\{111\} \langle 110 \rangle$, $\{111\} \langle 112 \rangle$, $\{112\} \langle 110 \rangle$, and $\{001\} \langle 110 \rangle$.

On the other hand, the obvious thermal activation process during hot rolling will instantly and significantly eliminate the work hardening induced by slips, so that the most easily activated $\{110\} \langle 111 \rangle$ systems can maintain continuous slip independently, and the systems such as $\{112\} \langle 111 \rangle$ and $\{123\} \langle 111 \rangle$ that require higher deformation stress to operate basically lose the opportunity to be activated. This adjustment in the crystallographic mechanism of plastic deformation will change the type of hot rolling texture^[9]. Furthermore, hot rolling deformation is usually completed at very high pass reductions, resulting in significant rotation of the principal rolling stress tensor around the transverse direction due to the additional large shear stress borne by the surface of the hot band, which in turn affects the texture type in the hot band surface^[12].

The formation of surface texture in GO steel hot band was simulated using the simple and intuitive Reaction Stress (RS) theory in plastic deformation crystallography^[10], where only the $\{110\} \langle 111 \rangle$ slip systems were activated and the principal stress tensor for rolling was rotated around the transverse direction for 42° induced by 40% pass reductions^[9]. The simulation results indicate that within the range of 78% to 97% of the total rolling reduction, the $\{110\} \langle 001 \rangle$ Goss texture consistently exhibits good stability in the surface of the hot band. Fig. 1 (d) shows the surface texture of the hot band when the simulated total deformation is 80%. The simulated tendency to form $\{112\} \langle 111 \rangle$ and $\{110\} \langle 001 \rangle$ textures is basically consistent with the actual observed results (Figs. 1 (a) and 1 (b)). Therefore, this simulation calculation has successfully traced the

deformation crystallographic process in the surface layer of the hot band.

2 Residual Goss Orientation and Its Stability After Cold Rolling and Annealing

Before the final secondary recrystallization, GO steel hot bands are subsequently subjected to cold rolling and recrystallization annealing processing. Special research has confirmed^[13] that the Goss single crystal, composed of Fe-3%Si, exhibits a large number of mutually parallel and thin flake-like microbands after cold rolling. Many microbands indicate low mis-orientation to their adjacent microbands, that is, they have low-angle grain boundaries around them. The orientation range of these microbands frequently includes $\{111\} \langle 112 \rangle$, $\{111\} \langle 110 \rangle$, and other non-Goss orientations. Goss orientation is unstable and the volume of Goss grains will decrease drastically during cold rolling. However, even after cold rolling up to 89% reduction, there are always a few sporadic thin flake-like Goss microbands, in most cases they are found embedded in two symmetrical $\{111\} \langle 112 \rangle$ microbands and surrounded by high-angle grain boundaries. Some opposite strains induced by deformation among adjacent microbands, for example between symmetric $\{111\} \langle 112 \rangle$ microbands can be appropriately relaxed and balanced by the in-between embedded Goss microbands^[14], which offers in turn limited stability for the Goss microbands. All thin flake like microbands have a thickness of less than $1 \mu\text{m}$ ^[13], which does not exceed the critical size necessary for recrystallization, therefore, they cannot grow directly as recrystallization nuclei during the recrystallization annealing.

The thermal activation of cold deformation is very weak and it is also difficult to implement rolling with a very large pass reduction. Therefore, both $\{112\} \langle 111 \rangle$ and $\{123\} \langle 111 \rangle$ slips will be activated simultaneously, and the principal stress tensor of rolling is also difficult to rotate obviously around the transverse direction. Fig.2 shows the rolling and recrystallization textures of a conventional GO steel from industrial processing with no obvious texture differences between center layer and surface layer. It can be seen that the cold rolling deformation of GO steel forms conventional textures such as $\{111\} \langle 110 \rangle$, $\{111\} \langle 112 \rangle$, $\{112\} \langle 110 \rangle$, and

$\{001\}\langle 110\rangle$ (Fig. 2 (a)), in comparison with Fig. 1 (c)). The unstable $\{112\}\langle 111\rangle$ texture did not appear after cold rolling, and the $\{110\}\langle 001\rangle$ Goss texture did not exhibit high stability as well. The very weak trace of Goss texture near the $\{110\}\langle 001\rangle$

orientation (Fig. 2 (a)), in comparison with Fig. 1 (c)) should originate mainly from Goss texture in the hot band surface, which may survive to a very limited extent after cold rolling^[13].

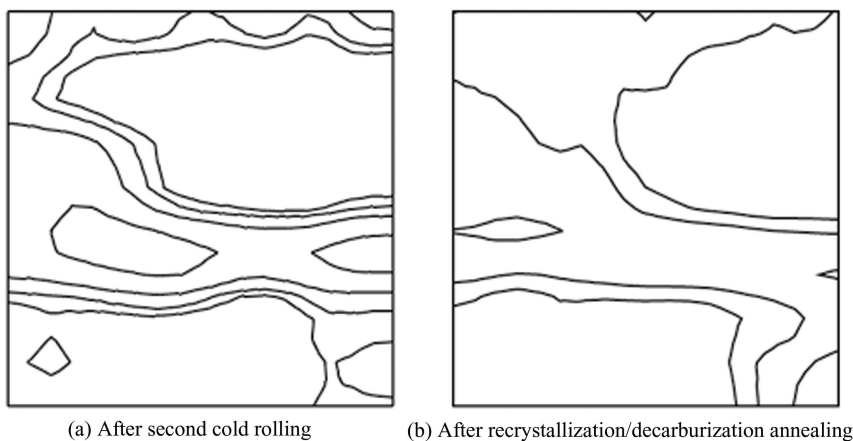


Fig.2 Experimental rolling and recrystallization textures of a conventional GO steel from industrial processing($\varphi_2=45^\circ$ ODF sections, density levels: 2, 4, 8)

Recrystallization is a process of nucleation and the spontaneous growth of recrystallization nuclei. Because almost all types of microbands have not yet reached the critical size for spontaneous growth after cold rolling^[13], there must be a nucleation process in the early stage of recrystallization annealing. The polygonization in the early stage of annealing is an important process to promote nucleation, during which many hardly mobile low-angle grain boundaries between microbands gradually disappear^[15]. When the size of sub-grains merged by the microbands gradually increases to exceed the critical value for spontaneous growth, and at the same time very mobile high-angle grain boundaries of the sub-grains are formed with the surrounding matrix, the sub-grains have transformed into recrystallization nuclei which will grow continuously in the later stage of recrystallization annealing. The close relationship between the recrystallization nuclei and the microbands within the deformed matrix results in a type of recrystallization texture similar to that of rolling texture (Fig. 2 (b)) after a very normal grain growth process. However, although Goss microbands already have very mobile high-angle grain boundaries, their small size does not allow for direct spontaneous growth, and the high-angle characteristic of the microband boundaries^[13] also hinders their nucleation process through polygonization^[15], resulting in the later appearance of Goss nuclei. This should also be why Goss grains

usually do not have the large size advantage after the primary recrystallization is complete. Nevertheless, recrystallization still slightly enhances the Goss texture (Fig. 2 (b)).

3 Molar Volume Effect During Precipitation of Inhibitor Particles

MnS and AlN particles are the main inhibitors in various GO steels, playing a crucial role in preventing non-Goss grain growth and only allowing Goss grain growth^[16]. The formation elements of MnS, AlN and other inhibitors first dissolve in the ferrite matrix, and then precipitate into fine particles dispersively in several thermal activation stages under supersaturation temperature conditions.

Based on the chemical structures of ferrite, MnS, and AlN, it can be inferred that when Mn, S, Al and other atoms in a solid solution state precipitate from ferrite, the ratio of the lost molar amount of the ferrite matrix to the newly formed molar amount of MnS and AlN is 1 : 0.5 and 1 : 1, respectively. The molar volumes of BCC ferrite, FCC MnS, and HCP AlN as well as the evolution with temperature, can be calculated based on their lattice constants and the corresponding temperature dependencies^[17-19]. Fig. 3 shows the calculated molar volume changes of ferrite, MnS, and AlN in the temperature range of 0 °C to 1600 °C. Considering the 1 : 0.5 molar ratio

relationship before and after MnS precipitation, half a molar volume of MnS was used in the figure. Obviously, the precipitation of MnS particles and AlN particles will induce significant volume expansion at all precipitation sites. Further calculations within the temperature range where abnormal grain growth behavior occurs in GO steel confirm that the volume expansion induced by MnS precipitation is always higher than 50%, and for AlN precipitation the volume expansion, it is even higher than 70%^[16]. Such significant precipitation expansion will inevitably have a very important impact on the precipitation behavior of these inhibitor particles.

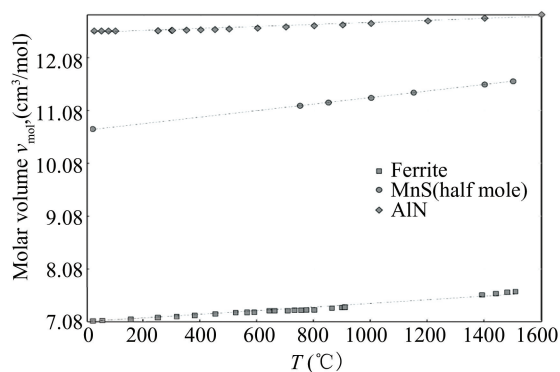


Fig. 3 Molar volume of MnS, AlN and ferrite matrix at different temperatures

4 Resistance Encountered by the Inhibitor Particles During Precipitation and Coarsening as well as the Differentiated Distribution of the Particles

The molar volume expansion effect generated during the precipitation process of inhibitors such as MnS and AlN causes precipitated particles to immediately experience compressive resistance from ferrite. Analysis shows^[16] that this compressive precipitation resistance increases exponentially with the increase of particle radius, so these particles have to always maintain a dispersed distribution and suppress the growth behavior of all grains. These particles will only lose their inhibition effect when they dissolve back into the ferrite matrix at much higher temperatures. The significant and stable molar volume expansion effect is also a key factor in the selection of MnS and AlN as the main inhibitors.

However, if the compressive resistance can be released to a certain extent, it will increase the chance of coarsening the precipitated particles. For example, in the grains near the free surface of a steel sheet, the

coarsening of precipitated particles will not be significantly hindered by the compressive resistance on the side facing the free surface, or at least the corresponding hindrance will be significantly reduced, thereby resulting in certain coarsening of surface particles and a decrease in their density. As the distance to the surface increases, the compressive resistance experienced by the precipitated particles will gradually increase until a critical depth or a deeper one is reached, at which point the coarsening resistance of the particles will reach a relatively high stable value, and the resistance in all directions will no longer exhibit significant depth dependence.

The inhibitor particles in conventional GO steels will precipitate during several heating processes, such as cooling, coiling, normalizing annealing of the hot bands, as well as intermediate annealing, recrystallization/decarburization annealing and temperature rise stage of secondary recrystallization annealing of the cold rolled sheets. The second phase particle densities in the surface and center layers of a conventional GO steel during industrial processes were statistically detected^[20], and the results confirm that the particle density of the surface layers was consistently lower than that of the corresponding center layers in hot band as well as after intermediate annealing, decarburization annealing and following annealing heated up to 875 °C of the cold rolled sheet (Fig. 4).

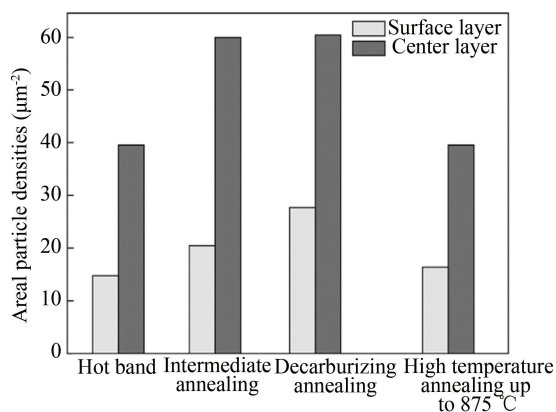


Fig. 4 Evolution of areal particle densities in the surface and center layers during industrial processes of a conventional GO steel

The compressive resistance induced by the molar volume effect near the surface layer of the steel sheet is more released, and the particles are prone to coarsening, which obviously reduces the particle density. It can be imagined that the closer to the surface, the lower the particle density. The lower

particle density corresponds to a lower inhibition effect, which is beneficial for the surface grains to grow earlier than those grains in the center layer during final secondary recrystallization annealing. The surface of the steel sheet is exactly where the initial Goss grains are located in GO steel^[8], which is of great significance for the formation of a strong Goss texture through abnormal grain growth during the secondary recrystallization process.

5 Elastic Anisotropy and Its Temperature Dependence of Ferrite

The ferrite of GO steels exhibits extremely strong anisotropy in elasticity. Taking the Young's modulus E as an example, ferrite has the lowest $E_{100} = 120$ GPa in the $\langle 100 \rangle$ direction, while it has the highest $E_{111} = 290$ GPa in the $\langle 111 \rangle$ direction^[21]. According to the phenomenological theory of first-order approximation^[1], the Young's modulus E_{uvw} (between 120 GPa and 290 GPa) of ferrite in any $[uvw]$ direction can be calculated. The Young's modulus in any direction on any crystal $\{hkl\}$ plane can also be confirmed when rotating 360° around the normal of the $\{hkl\}$ plane. There are four mutually non-parallel $\langle 111 \rangle$ directions with the highest Young's modulus in the body

centered cubic ferrite crystal, and the cross-product result of any two $\langle 111 \rangle$ directions is a $\langle 110 \rangle$ direction, which is the normal of a $\{110\}$ plane. Therefore, the $\{110\}$ plane is the only crystal plane in ferrite that contains two mutually non-parallel $\langle 111 \rangle$ directions and belongs to the most rigid crystal plane. Any other crystal plane will contain at most one $\langle 111 \rangle$ direction, such as the $\{112\}$ crystal plane.

Fig. 5 presents the calculated anisotropic Young's modulus E in any direction within several typical ferrite crystal planes, such as $\{110\}$, $\{112\}$, $\{111\}$, $\{221\}$, and $\{001\}$ during a 360° rotation around the normal direction of each crystal plane starting from a $\langle 110 \rangle$ direction in polar coordinates. The higher the Young's modulus E in one direction, the higher its rigidity. For example^[16], the E value in all directions within the $\{001\}$ plane is not higher than that in all directions within the $\{111\}$ or $\{112\}$ plane and belongs to the lowest rigidity crystal plane. There is a $\langle 111 \rangle$ direction within the $\{112\}$ plane, and during the 360° rotation, there are two places where the E value reaches the highest value (Fig.5, at 90° and 270°) in ferrite. There are two mutually non-parallel $\langle 111 \rangle$ directions within the most rigid $\{110\}$ plane, and during a 360° rotation, four of them reached the highest E value in ferrite.

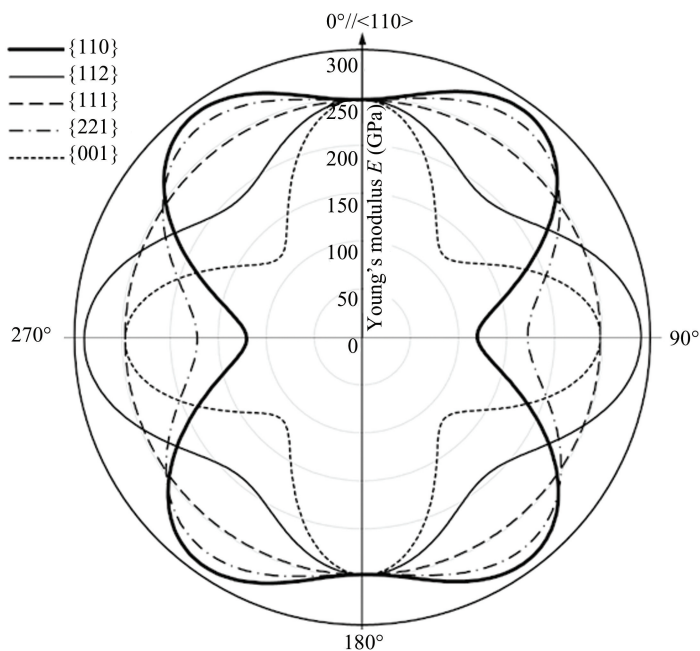


Fig.5 Fluctuations of Young's modulus E in different crystal planes and directions of ferrite at room temperature

The elastic anisotropy level of ferrite can be represented by $A = E_{111}/E_{100}$ ^[22], that is, the value of A is approximately equal to the ratio of the Young's

modulus between the highest stiffness $\langle 111 \rangle$ and the lowest stiffness $\langle 100 \rangle$. For ferrite at room temperature, $A = 290 \text{ GPa}/120 \text{ GPa} = 2.417$. Testing

and research in Ref.[23] have found that when ferrite is heated to around 900 °C where abnormal grain growth in GO steels begins, the elastic anisotropy parameter A value increases from 2.417 at room temperature to a level of 7.4, which will inevitably further significantly enhance the elastic anisotropy.

As shown in Fig. 4, the inhibitor particles in the surface and center layers of GO steel sheets before secondary recrystallization exhibit a differentiated distribution state, since the free space outside the surface of the steel sheet can hardly cause any particle coarsening resistance which may lead to much lower particle density. Therefore, it can be understood that during the secondary recrystallization annealing process, the grains in the surface layer of the annealing sheet usually grow more preferentially than those in the center layer.

The coarsening resistance of the particles near the sheet surface mainly comes from the direction along the inward normal of the steel sheet and all in-plane directions (Fig. 5). The resistance to particle coarsening is not only due to the molar volume effect, but also closely related to the Young's modulus E of the ferrite matrix. When the molar volume effect remains constant, the higher the Young's modulus, the greater the coarsening resistance^[16]. Therefore, particles in the $\langle 111 \rangle$ direction of the highest rigidity of ferrite will obtain the maximum coarsening resistance. Imaging that (refer to Fig. 5) the crystal planes of surface grains parallel to the rolling surface may be $\{110\}$, $\{112\}$, $\{111\}$, $\{221\}$, or $\{001\}$ planes, then the $\{110\}$ plane parallel to the surface has four $\langle 111 \rangle$ in-plane directions within 360° , and the inhibitor particles on this plane are the most difficult to coarsen, while the $\{001\}$ plane parallel to the surface does not have $\langle 111 \rangle$ in-plane directions within 360° , but has four $\langle 100 \rangle$ in-plane directions with the lowest rigidity, therefore, the inhibitor particles on $\{001\}$ plane are the easiest to coarsen. The resistance to particle coarsening in other crystal planes is between these two situations. In view of this, compared with other grains with lower particle density near the surface, the surface Goss grains with $\{110\}$ planes parallel to the rolling plane tend to maintain the highest particle density before the start of secondary recrystallization behaviors and the onset of abnormal growth of numerous grains near the surface. This phenomenon will occur at a certain depth inward from the surface of the steel sheet, and the deeper

towards the interior of the steel sheet, the weaker the effect, until the effect completely disappears in the sheet center. It can be seen that it is the surface $\{hkl\}$ index dependent effect induced by the elastic anisotropy of ferrite that leads to the differential coarsening of inhibitor particles within surface grains with different orientations^[24].

6 Abnormal Growth Mechanism of Surface Goss Grains Without Large Size Advantage

During the final annealing process of a conventional GO steel from industrial processing, a steel sheet was heated to 875 °C and stopped before secondary recrystallization occurred. The densities of inhibitor particles in a Goss grain and its surrounding non-Goss grains (1 to 7) were observed and analyzed on the sheet surface (Fig. 6)^[24], which shows that the particle density value is significantly lower than that of the central layer, since the particles inside surface grains have a better chance of coarsening and reducing their density^[25]. At the same time, the particle density is about $38/\mu\text{m}^2$ inside the surface Goss grain, but in a much lower range of $17\text{--}26/\mu\text{m}^2$ inside those non-Goss grains^[26]. This should be related to the presence of multiple in-plane $\langle 111 \rangle$ directions with the highest rigidity within the $\{110\}$ plane of the surface Goss grains (Fig.5) and corresponding higher coarsening resistance of the particles.

Whether the grain grows normally or abnormally, the geometric principle of grain growth determines that the growth must be a process of large grains swallowing small grains. In the initial stage of the secondary recrystallization annealing process, when the grains in the central layer have not yet grown, the grains in the surface layer will grow first in a way where larger grains engulf smaller grains. At this point, when large-sized non-Goss grains in the surface engulf adjacent smaller Goss grains, the higher particle density within the Goss grains will obviously slow down the migration speed of grain boundaries. On the other hand, the surface Goss grains may also be adjacent to some smaller non-Goss grains with low particle density inside, so the migration speed of grains boundaries, will be much faster when Goss grains engulf these small grains. In such a situation where the surface Goss grains are being engulfed by larger grains and are simultaneously engulfing smaller grains in the surrounding area, there

will always be some Goss grains that are enlarging outward at a faster rate than they are being engulfed (as shown in Fig. 6), resulting in an overall increase in the size of the Goss grains. When the size of this Goss grain grows to become larger than all other surface grains during long-term annealing, it can then quickly and comprehensively engulf all surface grains^[27].

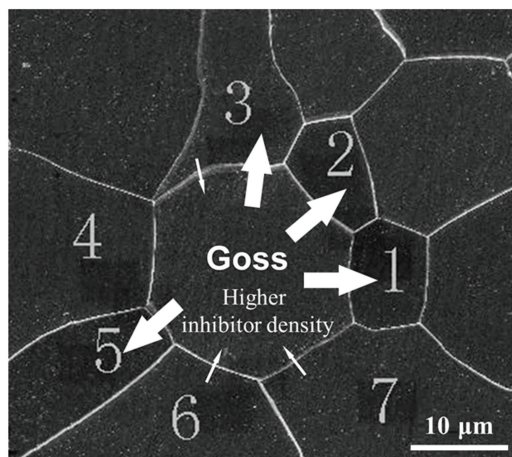


Fig.6 Boundary migration behaviors of surface grains and growth process of a Goss grain and 7 non-Goss grains observed in the sheet surface of a conventional GO steel from industrial processing (heated to 875 °C in the first stage of final secondary recrystallization annealing. The width of the white vectors is proportional to the speed of the corresponding grain boundary migration)

The basic abnormal growth process of Goss grains has been observed and described^[14]. The grain structure of Fig.6 was also observed in a sheet cross-section by means of EBSD (Electron Backscatter Diffraction) imaging (as shown in Fig.7), while the secondary recrystallization is about to start^[25]. It can be observed that while the vast majority of grains have not yet grown, a Goss grain (gray grain) connecting the surface of the steel sheet has already grown very large and demonstrated the ability to penetrate the steel sheet and engulf all other grains.

It is understandable that surface grains with lower particle density grow first, during which surface Goss grains with relatively higher particle density are more likely to rapidly expand into other grain areas of the steel sheet and gradually gain the advantage of larger size. In the later stage of secondary recrystallization annealing, when the temperature increases to such a level that all inhibitor particles dissolve into ferrite matrix and lose their role in pinning grain boundaries

while the size of the central layer grains is still very small, the already enlarged surface Goss grains then obtain the ability to penetrate the thickness of the steel sheet. Afterwards the oversized Goss grains can sweep across the entire steel sheet in the direction parallel to the sheet surface and ultimately become dominant after the secondary recrystallization.

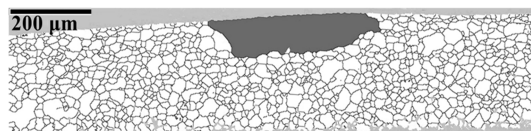


Fig.7 EBSD imaging showing grain structure in a sheet cross-section heated up to 875 °C while the secondary recrystallization is about to start (gray grain is Goss grain)

7 Summary

The effect of thermal activation on eliminating work hardening makes $\{110\} \langle 111 \rangle$ slip, which is most easily activated, the main crystallographic mechanism for hot deformation, while hot rolling with large pass reductions leads to the formation of a stable Goss texture in the surface layer of the hot band. During cold rolling, Goss grains can balance the strain incompatibility between non-Goss orientations, which allows a limited amount of Goss substructures to survive after the cold rolling deformation. The high angle grain boundary characteristics of the Goss substructures will delay their transformation into recrystallization nuclei, so Goss grains do not have the advantage of large size after the primary recrystallization. The molar volume expansion effect in the ferrite matrix makes it difficult for MnS and AlN particles to coarsen which suppresses grain growth process. However, in the surface layer of the steel sheet, the weakening of the expansion effect allows the density of these particles to be reduced to a certain extent through possible coarsening, which offers the preferential growth of surface grains. The very strong elastic anisotropy of ferrite at high temperatures leads to a higher particle density in those surface grains of which the $\{110\}$ plane is parallel to the rolling plane, including in surface Goss grains, than that in the surface non-Goss grains, which promotes the advantage of surface Goss grains growing first. The inhibitor particles dissolve into ferrite matrix and lose their role in pinning grain boundaries as the secondary recrystallization temperature

increases further in the subsequent stage. With an absolute size advantage, the Goss grains then obtain dominancy by engulfing all other grains. Moreover, the secondary recrystallization mechanism of GO steel provided here also explains or overcomes all the questions or challenges faced in existing related theories.

Acknowledgements

The author is grateful for the helpful discussion provided by Prof. Bevis Hutchinson from Swerim AB.

References

- [1] Mao W, Yang P. *Material Science Principles in Electrical Steels*. Beijing: Higher Education Press, 2013: 95 – 96, 137–140, 415–417.
- [2] Afer H, Rouag N, Penelle R. Comparison between the growth behaviour of the small Goss grains and that of the large matrix grains in silicon steels. Influence of the textured cluster presence. *Materials Science Forum*, 2005, 495–497: 525–530.
- [3] Chen N, Zaefferer S, Lahn L, et al. Effects of topology on abnormal grain growth in silicon steel. *Acta Materialia*, 2003, 51 (6) : 1755 – 1765. DOI: 10.1016/S1359 – 6454 (02) 00574–8.
- [4] Shimizu R, Harase J. Coincidence grain boundary and texture evolution in Fe-3% Si. *Acta Metallurgica*, 1989, 37 (4) : 1241–1249. DOI: 10.1016/0001–6160(89)90118–1.
- [5] Hayakawa Y, Szpunar J A. A new model of Goss texture development during secondary recrystallization of electrical steel. *Acta Materialia*, 1997, 45 (11) : 4713 – 4720. DOI: 10.1016/S1359–6454(97)00111–0
- [6] Park H, Kim D Y, Hwang N M, et al. Microstructural evidence of abnormal grain growth by solid-state wetting in Fe-3% Si steel. *Journal of Applied Physics*, 2004, 95 (10) : 5515–5521. DOI: 10.1063/1.1712012
- [7] Mao W, An Z, Li S. Influence of MnS particles on the behaviors of grain boundary migration in Fe-3% Si alloys. *Chinese Science Bulletin*, 2009, 54: 4537 – 4540. DOI: 10.1007/s11434–009–0607–3
- [8] Böttcher A, Lücke K. Influence of subsurface layers on texture and microstructure development in RGO electrical steel. *Acta Metallurgica et Materialia*, 1993, 41 (8) : 2503 – 2514. DOI: 10.1016/0956–7151(93)90331–L
- [9] Mao W, Li Y, Jin Z, et al. The initial source of Goss oriented grains in oriented electrical steels. *Journal of Inner Mongolia University of Science and Technology*, 2025, 44(1) : 1–7, 34. DOI : 10.16559/j.cnki.2095–2295.2025.01.001.
- [10] Mao W. *Plastic Deformation Crystallography of Metal Materials*. Beijing: Science Press, 2022: 145–148.
- [11] Heller M, Gibson J, Pei R, et al. Deformation of μm - and mm-sized Fe₂4wt%Si single- and bi-crystals with a high angle grain boundary at room temperature. *Acta Materialia*, 2020, 194: 452 – 463. DOI: 10.1016/j.actamat.2020.04.011
- [12] Mao W, Sun Z. Inhomogeneity of rolling texture in Fe-28Al-2Cr Alloy. *Scripta Materialia*, 1993, 29: 217–220.
- [13] Dorner D, Zaefferer S, Raabe D. Retention of the Goss orientation between microbands during cold rolling of an Fe₃%Si single crystal. *Acta Materialia*, 2007, 55 (7) : 2519–2530. DOI: 10.1016/j.actamat.2006.11.048
- [14] Mao W, Ren H. *Physical Metallurgical Principles of Grain Oriented Electrical Steels*. Beijing: Science Press, 2026: 97–100, 70–75.
- [15] Haasen P. *Physical Metallurgy*. Cambridge: Cambridge University Press, 1978: 350–353.
- [16] Mao W, Ren H. The mechanism of abnormal growth of Goss oriented grains during secondary recrystallization of oriented electrical steels. *Journal of Inner Mongolia University of Science and Technology*, 2025, 44 (2) : 111–118.
- [17] Yong Q. *Secondary Phases in Steels*. Beijing: Metallurgical Industry Press, 2006: 60–62.
- [18] Cui Z, Zhu L, Zhang Q, et al. Morphology analyses of MnS inclusions in 45 steel. *Foundry Technology*, 2016, 37(5) : 857–859.
- [19] Reeber R R, Wang K. Lattice parameters and thermal expansion of important semiconductors and their substrates. *Materials Research Society Symposium*, 2000, 622: T6.35.1–T6.35.6. DOI: DOI: 10.1557/PROC–622–T6.35.1
- [20] Li Y, Mao W, Yang P. Inhomogeneous distribution of second phase particles in grain oriented electrical steels. *Journal of Materials Science and Technology*, 2011, 27(12) : 1120–1124. DOI: 10.1016/S1005–0302(12)60006–1.
- [21] Schwintowski H P. *Wettbewerbs – und Kartellrecht (5. Auflage)*. Berlin: Springer-Verlage, 1994: 102–107.
- [22] Schwintowski H P. *Wettbewerbs – und Kartellrecht (2. Auflage)*. Berlin: Springer-Verlage, 1991: 84–87.
- [23] Routbort J L, Reid C N, Fisher E S, et al. High-temperature elastic constants and the phase stability of silicon-iron. *Acta Metallurgica*, 1971, 19: 1307–1316.
- [24] Mao W, Li Y, Guo W, et al. Influence of MnS particles inside grains on the boundary migration before secondary recrystallization of grain oriented electrical steels. *Solid State Phenomena*, 2010, 160: 247–250.
- [25] Mao W, Li Y, Yang P, et al. Abnormal growth mechanisms of Goss grains in grain-oriented electrical steels. *Materials Science Forum*, 2011, 702 – 703: 585 – 590. DOI: 10.4028/www.scientific.net/MSF.702–703.585
- [26] Guo W, Mao W. Abnormal growth of Goss grains in electrical steels. *Journal of Materials Science and Technology*, 2010, 26 (8) : 759 – 762. DOI: 10.1016/S1005–0302(10)60120–X
- [27] Mao W, Guo W, Li Y. Growth process of Goss grains during secondary recrystallization of grain-oriented electrical steels. *Steel Research International*, 2010, 81 (12) : 1117–1120. DOI: 10.1002/srin.201000051.